Radiochemical analysis of rubble collected from around and inside reactor buildings at Units 1 to 4 in Fukushima Daiichi Nuclear Power Station

Yoshiyuki Sato[1,2], Ryuji Aono[1,2], Miki Konda[1], Kiwamu Tanaka[1,2], Takashi Ueno[1,2], Ken-ichiro Ishimori[1,2], Yutaka Kameo[1,2]

[1]Japan Atomic Energy Agency, Tokai-mura, Ibaraki-ken 319-1195, Japan
[2] International Research Institute for Nuclear Decommissioning, Minato-ku, Tokyo 105-0003, Japan

Abstract

A large amount of contaminated rubble were generated by the accident at the Fukushima Daiichi Nuclear Power Station (F1NPS). For safe decommissioning of F1NPS, it is important to evaluate the composition and concentration of radionuclides in the rubble. To characterize the rubble collected at F1NPS, radiochemical analysis was operated. From the rubble collected from reactor buildings, ^{3}H, ^{14}C, ^{60}Co, ^{79}Se, ^{90}Sr, ^{99}Tc, ^{129}I, ^{137}Cs, ^{154}Eu, $^{238, 239+240}$Pu, ^{241}Am, and ^{244}Cm were detected. Radioactivity concentrations of ^{94}Nb and ^{152}Eu were below than the detection limit, as a result of analyzing all samples. The radioactivity concentration of ^{60}Co and ^{90}Sr depended on that of ^{137}Cs. The rubble collected from reactor building at Unit 1 of 1st floor and 5th floor had similar radioactive ratio of ^{90}Sr/^{137}Cs and ^{60}Co/^{137}Cs. The radioactive ratio of ^{90}Sr/^{137}Cs were similar between the rubble collected from reactor building of 1st floor and 5th floor. This result implied that regardless of sampling location in reactor building, the radioactive ratio of ^{90}Sr/^{137}Cs were consistence. This analysis was characterized the radioactivity concentrations of rubble.

1. Introduction

Fukushima Daiichi Nuclear Power Station (F1NPS) was severely damaged by hydrogen explosions resulting from the tsunami caused by the Great East Japan Earthquake that occurred on 11 March 2011. After the accident, radionuclides, including ^{137}Cs and ^{90}Sr, were released from reactor buildings at Units 1 to 3, and released radionuclides contaminated large amount of rubble. As of 30 June 2017, 210,500 m^3 of contaminated rubble was stored [1] at the F1NPS site. The rubble was generated mainly by the collapse and dismantling of reactor buildings. To examine a strategy for treatment and subsequent disposal of the rubble, it was essential to clarify their radionuclide and radioactivity concentration. In order to clarify the contamination of rubble, it is necessary to analyze alpha and beta nuclides that are difficult to measure as well as to analyze gamma nuclides.

In previous research, we developed analytical methods for radioactive waste generated by research institute [2]. Based on these analytical methods, we also analyzed radioactive waste generated at the F1NPS site, such as contaminated water, cutting trees, and rubble. Almost these radioactive wastes were collected from around reactor buildings [3, 4], and their analytical data were utilized for environmental improvement of F1NPS site. In the decommissioning of F1NPS, removal of the rubble in reactor buildings and dismantling of reactor buildings began. As the decommissioning of reactor buildings progresses, a large amount of radioactive waste will be generated from inside reactor buildings. Therefore, analysis of the rubble collected from inside reactor buildings is necessary to prevent exposure of workers and to decide disposal of the rubble. In order to accelerate decommissioning as well as disposal of the contaminated rubble, it is necessary to acquire detailed radioactivity data.

In this study, we analyzed rubble collected from fifth floor of the reactor building of Unit 1 and first floor of the reactor buildings of Units 1 and 3. The nuclides analyzed were ^{3}H, ^{14}C, ^{60}Co, ^{63}Ni, ^{79}Se, ^{90}Sr, ^{94}Nb, ^{99}Tc, ^{129}I, ^{137}Cs, ^{152,154}Eu, $^{238,239+240}$Pu, ^{241}Am, and ^{244}Cm. The radioactivity concentrations of the rubble collected from the F1NPS obtained by radiochemical analysis are

reported. From the radioactivity concentrations of the rubble, the characteristics of the rubble generated by the F1NPS accident are discussed.

2. Experimental

2. 1. Samples

Three samples were collected from around reactor buildings at Units 1, 3 and 4. Sampling location where three samples were collected was shown in previous study [3]. Twenty eight samples were collected from inside reactor buildings at Units 1 and 3 by a remote-control device. The sampling locations of samples collected from 1st floor of reactor buildings at Units 1 and 3 and 5th floor of reactor buildings at Unit 1 are shown in Figure 1 and 2 respectively. Information such as the dose rate and weight of the collected rubble is summarized in Table 1. The samples were transported from the F1NPS to the Nuclear Science Research Institute of the JAEA for measurement.

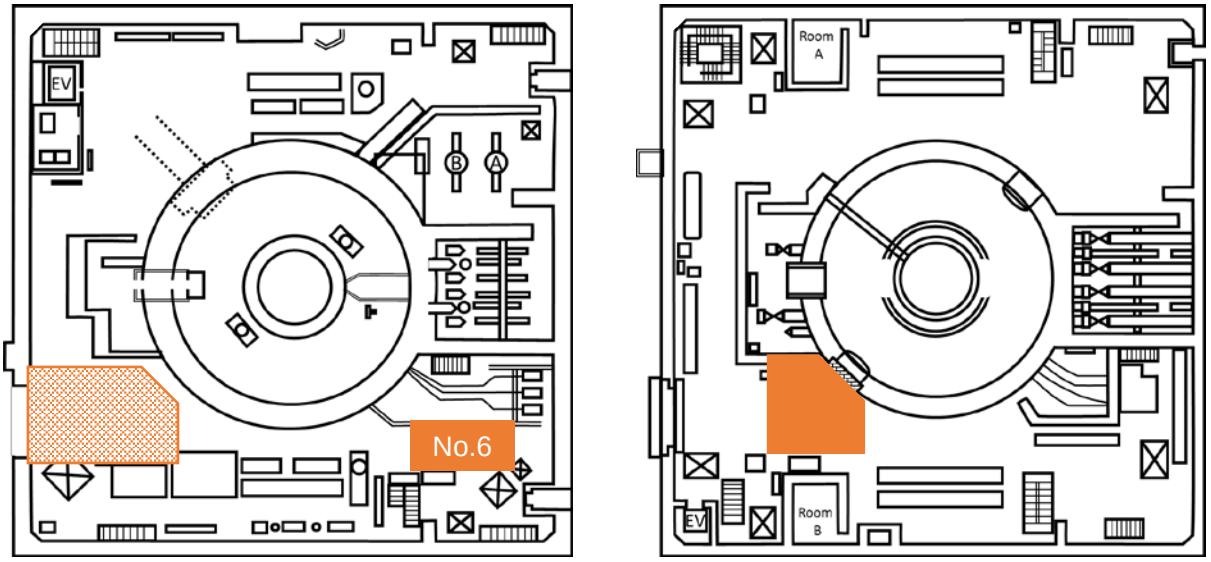

1st floor of reactor buildings at Unit 1
Sampling location of sample No.4 and 5

1st floor of reactor buildings at Unit 3
Sampling location of sample No.7-11

Figure 1 Sampling locations of rubble samples collected from 1st floor of reactor buildings at Units 1 and 3 in F1NPS.

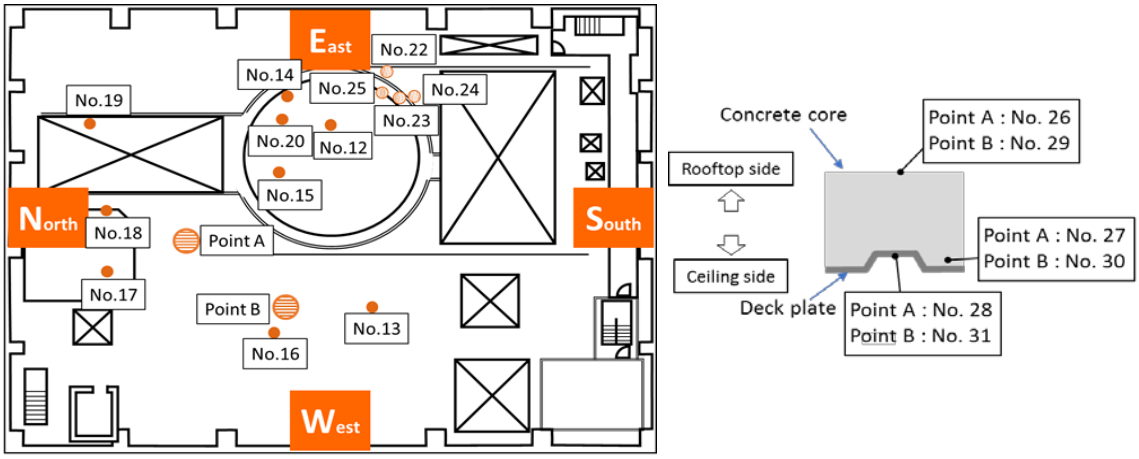

Sample No. 21(RB-CR-R10) : extraneous matter collected from the sampler

Figure 2 Sampling locations of rubble samples collected from 5th floor of reactor building at Unit 1 in F1NPS.

Table 1 Description of samples analyzed in this study

No.	Sample	Sampling Date	Form	One centimeter dose equivalent rate (μSv/h)	Weight (g)
1	1U-05	July 2012	Massive (fist size), including ash-colored coating material	14.0	50.0
2	3U-03	June 2012	Massive (fist size), including aqua-colored coating material	52.0	49.9
3	4U-07	June 2012	Grain geometry, including aqua-colored coating material	B.G.	50.4
4	1RB-AS-R2	October 2013	Concrete	32	4
5	1RB-AS-R9	October 2013	Concrete	52	5
6	1RB-DE-C1	February 2014	Surface paint	14	10
7	3RB-AS-R1	March 2014	Concrete	22	25
8	3RB-AS-R2	March 2014	Concrete	57	17
9	3RB-AS-R5	March 2014	Concrete	25	24
10	3RB-AS-R7	March 2014	Concrete	31	9
11	3RB-AS-R10	March 2014	Concrete	30	15
12	1RB-CR-R1	October 2015	Concrete	30	1.4
13	1RB-CR-R2	October 2015	Concrete	18	1.5
14	1RB-CR-R3	October 2015	Concrete	7.5	1.1
15	1RB-CR-R4	October 2015	Concrete	38	1.2
16	1RB-CR-R5	October 2015	Concrete	9.0	2.1
17	1RB-CR-R6	October 2015	Concrete	44	1.6
18	1RB-CR-R7	October 2015	Concrete	23	1.2
19	1RB-CR-R8	October 2015	Concrete	45	1.2
20	1RB-CR-R9	October 2015	Concrete	8.0	1.5
21	1RB-CR-R10	October 2015	Concrete	3.5	0.6
22	1RB-CR-R11	October 2015	Concrete[1)]	35	0.5
23	1RB-CR-R12	October 2015	Concrete[1)]	65	0.4
24	1RB-CR-R13	October 2015	Concrete[1)]	150	0.1
25	1RB-CR-R14	October 2015	Concrete[1)]	45	0.1
26	1RB-OP-C1-1	April 2016	Concrete	4.2	5.46
27	1RB-OP-C1-2	April 2016	Concrete	130	5.67
28	1RB-OP-D1-1	April 2016	Surface paint[2)]	980	0.54
29	1RB-OP-C2-1	April 2016	Concrete	2.3	5.50
30	1RB-OP-C2-2	April 2016	Concrete	4.3	6.16
31	1RB-OP-D2-1	April 2016	Surface paint[2)]	25	0.55

1) Collected from under the collapsed roof
2) Core boring sample of the collapsed roof

The pretreatment and analytical procedure for sample No.1-3 and No.4-11 is shown in the report before last [3] and the previous report respectively [4].

Sample No. 12-24 were collected as granulated concretes which were sufficiently fine to analyze. The quantity of these concrete samples was not enough to divide into the portions analyzing 17 nuclides. Therefore, these concrete samples were classified into four groups according to sampling location to analyze 17 nuclides. Figure 2 shows sampling locations of rubble samples collected from 5th floor of reactor building at Unit 1 in F1NPS. Sample No. 12, 14, 15, and 20 were classified into the rubble collected from around the reactor well. Sample No. 13 and 16 were classified into the rubble collected from west side of the 5th floor. Sample No. 17, 18 and 19 were classified into the rubble collected from north side of the 5th floor. Sample No. 21, 22, 23 and 24 were classified into the rubble collected from under the collapsed roof. Each grouped samples were assigned two portions according to chemical separation. One portion was conducted acid dissolution with microwave heating method. The other one was divided into six portions, and these six portions were conducted alkaline fusion method or

combustion method. Sample No. 12-24 was difficult to divide according to sample weight, since these samples were small quantity. Therefore, after the radioactivity of the whole sample was measured, the radioactivity of the part sample obtained by dividing the whole sample into portions was measured. Since the weight ratio and the radioactivity ratio of the part sample to the whole sample were almost the same ratio, it was confirmed that the sample weight depended on radioactivity.

Sample No. 25-31 were the surface paints of boring core which were bored the collapsed roof. These surface paint samples were cut finely to analyze. To confirm that there was no significant deviation in the radio activity concentrations of the subdivided rubble, ^{137}Cs concentration was measured using a high-purity Ge detector (HPGe, SEIKO EG&G CO., LTD.).

2. 2. Outline of experimental procedure

These samples shown in Table 1 were analyzed radioactivity concentrations of gamma-ray-emitting nuclides ^{60}Co, ^{94}Nb, ^{137}Cs, and $^{152,154}Eu$, beta-particle-emitting nuclides ^{3}H, ^{14}C, ^{79}Se, ^{90}Sr, ^{63}Ni, ^{99}Tc, and ^{129}I, and alpha-particle-emitting nuclides ^{238}Pu, $^{239+240}Pu$, ^{241}Am, and ^{244}Cm. Sample No. 12-31 were conducted according to the analytical procedure shown in Figure 3. Among the analytical procedures for these samples, the analytical procedure that changed the procedure of the previous report is outlined in the following section.

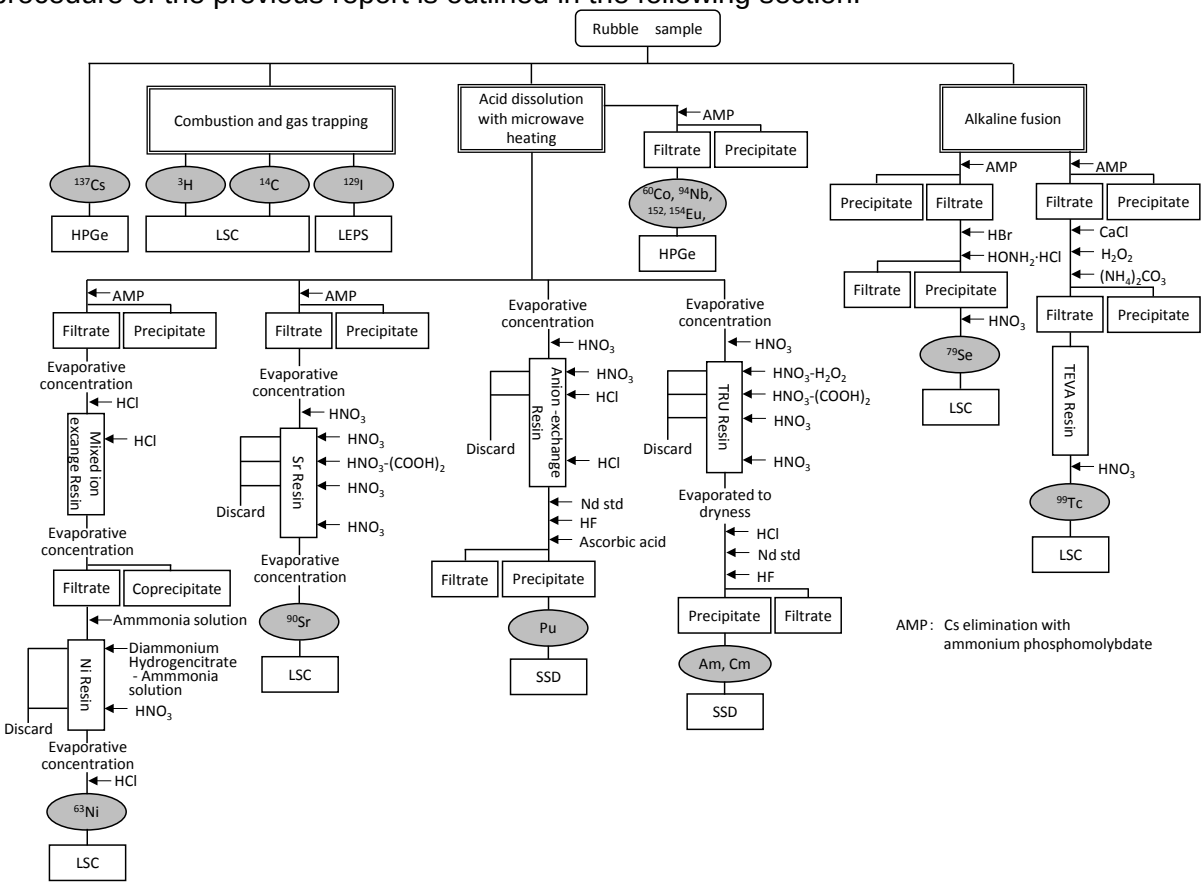

Figure 3. Flowchart for analysis of ^{3}H, ^{14}C, ^{60}Co, ^{63}Ni, ^{79}Se, ^{90}Sr, ^{94}Nb, ^{99}Tc, ^{129}I, ^{137}Cs, ^{152}Eu, ^{154}Eu, and alpha-particle-emitting nuclides in rubble samples collected at the F1NPS.

2. 2. 1 Analysis of ^{129}I

A schematic of combustion apparatus for analysis of ^{129}I is shown in Figure 4. 1 M NaOH solution was added to the impingers. Quartz wool and hopcalite II were placed in a quartz tube, and the quartz tube was placed in a tubular electric furnace and heated in the same procedure as in the previous report. There are two chemical form, I^- and IO_3^-. In the case of measuring the sample by ICP-MS, the sensitivity of I^- is not stabilized due to memory effect from the instrument, and the sensitivity of IO_3^- is stable but lowered. Therefore, measurement with low

energy photon spectrometer (LEPS, SEIKO EG&G CO., LTD.) whose sensitivity is not dependent on chemical species was adopted, and the pretreatment was changed accordingly. Iodine carrier was added to the NaOH solution recovered from the impingers to produce silver iodide and centrifuged with a centrifugal separator. Concentrated aqueous ammonia was added to the separated precipitate, and a precipitate derived from sodium hydrogen sulfite was dissolved, followed by suction filtration. After the precipitation drying, the sample was measured with LEPS.

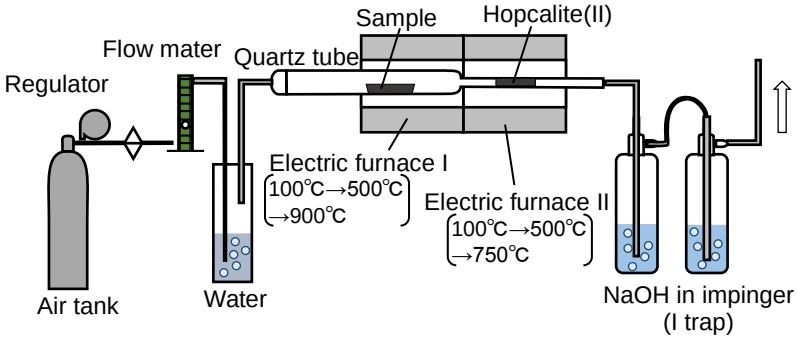

Figure 4 Schematic of combustion apparatus for analysis of ^{129}I

2. 2. 2 Analysis of ^{241}Am, ^{244}Cm

The acid dissolved solution of rubble sample was separated by a TRU resin column in the same way as in the previous report. A neodymium carrier and hydrofluoric acid were added to the Am and Cm fraction. The neodymium carrier-added sample solution was suction filtered, and the fluoride precipitate was washed with purified water. The dried membrane filter was fixed to a Ta plate and the radioactivity of ^{241}Am and ^{244}Cm of the sample was measured with a silicon surface barrier detector (SSD, SEIKO EG&G CO., LTD.).

In the previous report, the measurement sample solution was baked on a Ta plate to make it as a measurement sample. However, it is difficult to prepare the same thickness sample constantly and the influence of self absorption is large. Therefore, the method for preparing the measurement sample was changed, and the NdF_3 coprecipitation was recovered by filtration and used as a measurement sample.

2. 2. 3 Analysis of $^{238, 239+240}Pu$

In the previous paper, Pu was separated with UTEVA resin that is useful in isolating the target product. However, to cope with the analysis sample containing unexpected elements, iron coprecipitation and anion exchange resin was selected. The acid dissolved solution of rubble sample was fractionated for spiked sample and non-spiked sample. A ^{242}Pu solution was added to the sample for spike. Iron carrier was added to both spiked sample and non-spiked sample. The iron carrier-added sample solution was heated and concentrated to about 1 mL. After flowing of the concentrated sample solution, nitric acid and then hydrochloric acid were passed through the anion exchange column, 1 M hydrochloric acid was passed through the column, and the Pu fraction was recovered. A neodymium carrier and hydrofluoric acid were added to the Pu fraction. The neodymium carrier-added sample solution was suction filtered, and the fluoride precipitate was washed with purified water. The dried membrane filter was fixed to a Ta plate and the radioactivity of $^{238, 239+240}Pu$ of the sample was measured with a SSD. Also, as in the analytical procedure of ^{241}Am, ^{244}Cm, the NdF_3 coprecipitation was recovered by filtration and used as a measurement sample.

3. Result and Discussion

3.1. Characteristics of rubble at each sampling location in Unit 1

The radioactivity concentrations of the gamma-ray-emitting, beta-particle-emitting, alpha-particle-emitting nuclides on 11 March 2011 in the rubble are tabulated in Table 2, 3, 4, and 5. The average radioactivity ratio $\overline{x}$ were calculated based on a computational expression as follows.

$$\overline{y} = \frac{1}{n}\sum_{i=1}^{n} \log x_i \qquad (1)$$

$$\overline{x} = 10^{\overline{y}} \qquad (2)$$

Where x and $\overline{y}$ are the radioactivity ratio of each sample, and arithmetic average of logarithmic value, respectively. The average radioactivity ratios were including previous study [3, 4]. Correlation between ^{137}Cs and radio isotopes was evaluated by t-test. At this section, we discussed Characteristics of rubble at each sampling location in Unit 1. Therefore, the sample No. 4 - 6 and 12- 31 were compared according to difference of sampling floor.

Table 2 shows that ^{137}Cs was detected in all rubble and was distributed between 1.2×10^{3} and 1.5×10^{7} Bq/g in the rubble collected from 5th floor in Unit 1. Except two rubble, Co-60 was detected all rubble was distributed between 2.8×10^{-1} and 2.3×10^{2} Bq/g in the rubble collected from 5th floor. Europium-154 was detected in only rubble collected from 5th floor, was distributed between 1.9×10^{0} and 5.2×10^{1} Bq/g, and the others were content below the detection limit. Niobium-94 and Europium-152 were content below the detection limit in all rubble.

Table 3 shows that ^{90}Sr was detected in all rubble and was distributed between 2.3×10^{0} and 4.5×10^{3} Bq/g in the rubble collected from 5th floor in Unit 1. Moreover ^{63}Ni distributed between 2.3×10^{0} and 3.7×10^{1} Bq/g. Selenium-79 and technetium-99 were detected in rubble collected from under the roof and were distributed between 2.9×10^{-1} and 6.5×10^{0} Bq/g, and 1.3×10^{-1} and 2.3×10^{0} Bq/g, respectively, and the others were content below the detection limit. The rubble collected from under the roof were higher radioactivity concentration than that collected from surface of the roof. However radioactivity ratios ^{60}Co to ^{137}Cs, ^{63}Ni to ^{137}Cs, and ^{90}Sr to ^{137}Cs were constant regardless of sampling location on the 5th floor. Comparison of rubble collected from the 5th floor with that collected from the 1st floor, ^{60}Co/^{137}Cs, and ^{90}Sr/^{137}Cs radioactivity ratio of the 5th floor was no less high than that of the 1st floor. In addition, radioactivity concentration of ^{60}Co and ^{90}Sr were correlation to that of ^{137}Cs according to t-test. These results showed radioactivity ratios of involatile nuclides to ^{137}Cs were constant regardless of sampling location at Unit 1.

Table 4 shows radioactivity concentrations of volatile nuclides. Tritium was detected in all rubble was distributed between 5.0×10^{-1} and 3.3×10^{2} Bq/g in the rubble collected from the 5th floor in Unit 1. Carbon-14 was detected in all rubble except for one rubble, was distributed between 3.4×10^{-1} and 3.7×10^{1} Bq/g in the rubble collected from the 5th floor. Iodine-129 was detected in four samples collected from Unit 1 and was distributed between 3.0×10^{-1} and 2.3×10^{1} Bq/g. Radioactivity ratio of ^{3}H to ^{137}Cs, and ^{14}C/^{137}Cs varied widely ranging three orders of magnitude however radioactivity concentrations of ^{3}H and ^{14}C were correlation to that of ^{137}Cs according to t-test. In general, Radioactivity concentration of ^{3}H and ^{14}C in radioactive waste were not depend on that of ^{137}Cs since ^{3}H and ^{14}C diffused while repeating adsorption and desorption as gas (i.e. water vapor or carbon dioxide) [5]. We did not conclude that radioactivity concentration of ^{3}H and ^{14}C depended on that of ^{137}Cs since chemical property of ^{137}Cs was differ from that of ^{3}H and ^{14}C these were volatile at common temperature. The analysis of rubble samples should continue and the results should be compared to the calculated data to further refine the figures determined this work.

Table 5 shows radioactivity concentrations of alpha-particle-emitting nuclides. Radioactivity

concentration of these five nuclides in the rubble collected from inside of rector buildings were ranged same order of magnitude. Radioactivity ratios of these five nuclides to ^{137}Cs were similar to those analyzed in previous study [3, 4]. These results showed radioactivity ratios of alpha-particle-emitting nuclides to ^{137}Cs were constant regardless of sampling location at Unit 1 as was the case with $^{90}Sr/^{137}Cs$ ratios and $^{60}Co/^{137}Cs$ ratios.

Table 2 Concentrations of gamma-ray-emitting nuclides on 11 March 2011 (Bq/g).

No.	Sample	^{60}Co	^{94}Nb	^{137}Cs	^{152}Eu	^{154}Eu
1	1U-05	$< 2\times10^{-1}$	$< 5\times10^{-1}$	$(1.4\pm0.1)\times10^{3}$	$< 6\times10^{-1}$	$< 6\times10^{-1}$
2	3U-03	$(2.7\pm0.9)\times10^{-1}$	$< 5\times10^{-1}$	$(1.5\pm0.1)\times10^{4}$	$< 6\times10^{-1}$	$< 6\times10^{-1}$
3	4U-07	$< 2\times10^{-1}$	$< 5\times10^{-1}$	$(6.6\pm0.1)\times10^{0}$	$< 6\times10^{-1}$	$< 6\times10^{-1}$
4	1RB-AS-R2	$(1.1\pm0.1)\times10^{0}$	$< 7\times10^{-2}$	$(1.1\pm0.1)\times10^{5}$	$< 7\times10^{-1}$	$< 3\times10^{-1}$
5	1RB-AS-R9	$(1.4\pm0.1)\times10^{0}$	$< 7\times10^{-2}$	$(1.8\pm0.1)\times10^{5}$	$< 7\times10^{-1}$	$< 3\times10^{-1}$
6	1RB-DE-C1	$(2.8\pm0.4)\times10^{-1}$	$< 7\times10^{-2}$	$(1.7\pm0.1)\times10^{4}$	$< 7\times10^{-1}$	$< 3\times10^{-1}$
7	3RB-AS-R1	$(7.0\pm0.5)\times10^{-1}$	$< 7\times10^{-2}$	$(1.4\pm0.1)\times10^{4}$	$< 7\times10^{-1}$	$< 3\times10^{-1}$
8	3RB-AS-R2	$(7.7\pm0.5)\times10^{-1}$	$< 7\times10^{-2}$	$(5.0\pm0.1)\times10^{4}$	$< 7\times10^{-1}$	$< 3\times10^{-1}$
9	3RB-AS-R5	$(2.9\pm0.4)\times10^{-1}$	$< 7\times10^{-2}$	$(1.9\pm0.1)\times10^{4}$	$< 7\times10^{-1}$	$< 3\times10^{-1}$
10	3RB-AS-R7	$(2.9\pm0.1)\times10^{0}$	$< 7\times10^{-2}$	$(5.7\pm0.1)\times10^{4}$	$< 7\times10^{-1}$	$< 3\times10^{-1}$
11	3RB-AS-R10	$(5.4\pm0.5)\times10^{-1}$	$< 7\times10^{-2}$	$(3.0\pm0.1)\times10^{4}$	$< 7\times10^{-1}$	$< 3\times10^{-1}$
12	1RB-CR-R1	–	–	$(2.8\pm0.1)\times10^{5}$	–	–
13	1RB-CR-R2	$(2.3\pm0.2)\times10^{0}$	$< 3\times10^{-1}$	$(1.5\pm0.1)\times10^{5}$	$< 3\times10^{0}$	$< 1\times10^{0}$
14	1RB-CR-R3	–	–	$(6.2\pm0.1)\times10^{4}$	–	–
15	1RB-CR-R4	$(9.1\pm0.3)\times10^{0}$	$< 3\times10^{-1}$	$(3.8\pm0.1)\times10^{5}$	$< 3\times10^{0}$	$(1.9\pm0.3)\times10^{0}$
16	1RB-CR-R5	–	–	$(4.7\pm0.1)\times10^{4}$	–	–
17	1RB-CR-R6	$(1.2\pm0.1)\times10^{1}$	$< 3\times10^{-1}$	$(3.1\pm0.1)\times10^{5}$	$< 3\times10^{0}$	$(2.5\pm0.3)\times10^{0}$
18	1RB-CR-R7	–	–	$(2.0\pm0.1)\times10^{5}$	–	–
19	1RB-CR-R8	$(1.1\pm0.1)\times10^{1}$	$< 3\times10^{-1}$	$(4.1\pm0.1)\times10^{5}$	$< 3\times10^{0}$	$(2.2\pm0.4)\times10^{0}$
20	1RB-CR-R9	–	–	$(5.8\pm0.1)\times10^{4}$	–	–
21	1RB-CR-R10	–	–	$(3.9\pm0.1)\times10^{4}$	–	–
22	1RB-CR-R11	–	–	$(8.2\pm0.1)\times10^{5}$	–	–
23	1RB-CR-R12	$(1.5\pm0.1)\times10^{1}$	$< 1\times10^{0}$	$(1.7\pm0.1)\times10^{6}$	$< 9\times10^{0}$	$< 4\times10^{0}$
24	1RB-CR-R13	$(1.6\pm0.1)\times10^{2}$	$< 4\times10^{0}$	$(1.5\pm0.1)\times10^{7}$	$< 4\times10^{1}$	$(2.1\pm0.4)\times10^{1}$
25	1RB-CR-R14	–	–	$(1.1\pm0.1)\times10^{7}$	–	–
26	1RB-OP-C1-1	$(8.1\pm1.2)\times10^{-1}$	$< 3\times10^{-1}$	$(9.0\pm0.1)\times10^{3}$	$< 2\times10^{0}$	$< 1\times10^{0}$
27	1RB-OP-C1-2	$(1.0\pm0.1)\times10^{1}$	$< 2\times10^{-1}$	$(4.2\pm0.1)\times10^{5}$	$< 2\times10^{0}$	$(2.1\pm0.3)\times10^{0}$
28	1RB-OP-D1-1	$(2.3\pm0.1)\times10^{2}$	$< 5\times10^{0}$	$(2.3\pm0.1)\times10^{6}$	$< 5\times10^{1}$	$(5.2\pm0.6)\times10^{1}$
29	1RB-OP-C2-1	$< 4\times10^{-1}$	$< 2\times10^{-1}$	$(1.2\pm0.1)\times10^{3}$	$< 2\times10^{0}$	$< 9\times10^{-1}$
30	1RB-OP-C2-2	$< 4\times10^{-1}$	$< 2\times10^{-1}$	$(1.0\pm0.1)\times10^{4}$	$< 2\times10^{0}$	$< 8\times10^{-1}$
31	1RB-OP-D2-1	$(8.8\pm0.3)\times10^{1}$	$< 4\times10^{0}$	$(7.4\pm0.1)\times10^{5}$	$< 4\times10^{1}$	$< 2\times10^{1}$

Table 3 Concentrations of beta-particle-emitting nuclides on 11 March 2011 (Bq/g).

No.	Sample	^{63}Ni	^{79}Se	^{90}Sr	^{99}Tc
1	1U-05	—	$< 5\times10^{-2}$	$(1.4\pm0.1)\times10^{0}$	$< 5\times10^{-2}$
2	3U-03	—	$< 5\times10^{-2}$	$(2.7\pm0.1)\times10^{-1}$	$< 5\times10^{-2}$
3	4U-07	—	$< 5\times10^{-2}$	$< 6\times10^{-2}$	$< 5\times10^{-2}$
4	1RB-AS-R2	—	—	$(1.3\pm0.1)\times10^{3}$	—
5	1RB-AS-R9	—	—	$(1.3\pm0.1)\times10^{3}$	—
6	1RB-DE-C1	—	$< 5\times10^{-2}$	$(7.0\pm0.1)\times10^{2}$	—
7	3RB-AS-R1	—	$< 5\times10^{-2}$	$(1.1\pm0.1)\times10^{1}$	$< 5\times10^{-2}$
8	3RB-AS-R2	—	$< 5\times10^{-2}$	$(2.5\pm0.1)\times10^{1}$	$(7.1\pm1.0)\times10^{-2}$
9	3RB-AS-R5	—	$< 5\times10^{-2}$	$(1.2\pm0.1)\times10^{1}$	$< 5\times10^{-2}$
10	3RB-AS-R7	—	$(7.0\pm1.1)\times10^{-2}$	$(1.2\pm0.1)\times10^{2}$	$(9.8\pm1.1)\times10^{-2}$
11	3RB-AS-R10	—	$< 5\times10^{-2}$	$(1.9\pm0.1)\times10^{1}$	$(5.8\pm1.0)\times10^{-2}$
12	1RB-CR-R1	—	$< 2\times10^{-1}$	—	$< 3\times10^{-1}$
13	1RB-CR-R2	—	—	$(5.6\pm0.2)\times10^{1}$	—
15	1RB-CR-R4	—	—	$(2.0\pm0.1)\times10^{2}$	—
16	1RB-CR-R5	—	$< 2\times10^{-1}$	—	$< 3\times10^{-1}$
17	1RB-CR-R6	$(2.3\pm0.1)\times10^{0}$	—	$(2.0\pm0.1)\times10^{2}$	—
18	1RB-CR-R7	—	$< 3\times10^{-1}$	—	$< 4\times10^{-1}$
19	1RB-CR-R8	—	—	$(2.2\pm0.1)\times10^{2}$	—
22	1RB-CR-R11	—	$< 9\times10^{-1}$	—	$< 9\times10^{-1}$
23	1RB-CR-R12	—	—	$(4.3\pm0.1)\times10^{2}$	—
24	1RB-CR-R13	$(2.7\pm0.1)\times10^{1}$	—	$(4.5\pm0.1)\times10^{3}$	—
25	1RB-CR-R14	—	$(6.5\pm1.4)\times10^{0}$	—	$< 7\times10^{0}$
26	1RB-OP-C1-1	—	$< 2\times10^{-1}$	$(1.1\pm0.1)\times10^{1}$	$< 2\times10^{-1}$
27	1RB-OP-C1-2	—	$(2.9\pm0.5)\times10^{-1}$	$(1.1\pm0.1)\times10^{3}$	$(1.3\pm0.4)\times10^{-1}$
28	1RB-OP-D1-1	$(3.7\pm0.2)\times10^{1}$	$(2.8\pm0.4)\times10^{0}$	$(1.9\pm0.1)\times10^{3}$	$(2.3\pm0.4)\times10^{0}$
29	1RB-OP-C2-1	—	$< 2\times10^{-1}$	$(2.3\pm0.1)\times10^{0}$	$< 2\times10^{-1}$
30	1RB-OP-C2-2	—	$< 2\times10^{-1}$	$(6.7\pm0.1)\times10^{0}$	$(1.5\pm0.3)\times10^{-1}$
31	1RB-OP-D2-1	$(1.3\pm0.1)\times10^{1}$	$< 2\times10^{0}$	$(1.3\pm0.1)\times10^{3}$	$< 2\times10^{0}$

Table 4 Concentrations of beta-particle-emitting volatile nuclides on 11 March 2011 (Bq/g).

No.	Sample	^{3}H	^{14}C	^{129}I
1	1U-05	$(8.5\pm1.6)\times10^{-2}$	$(3.9\pm0.2)\times10^{-1}$	$< 5\times10^{-2}$
2	3U-03	$(3.2\pm0.3)\times10^{-1}$	$(1.2\pm0.1)\times10^{0}$	$< 5\times10^{-2}$
3	4U-07	$(2.3\pm0.3)\times10^{-1}$	$(3.0\pm0.2)\times10^{-1}$	$< 5\times10^{-2}$
6	1RB-DE-C1	$(1.9\pm0.1)\times10^{0}$	$(2.1\pm0.2)\times10^{-1}$	—
7	3RB-AS-R1	$(5.3\pm0.2)\times10^{-1}$	$(2.2\pm0.2)\times10^{-1}$	$< 5\times10^{-2}$
8	3RB-AS-R2	$(8.7\pm0.2)\times10^{-1}$	$(1.5\pm0.2)\times10^{-1}$	$(5.2\pm0.1)\times10^{-2}$
9	3RB-AS-R5	$(6.4\pm0.2)\times10^{-1}$	$(1.4\pm0.2)\times10^{-1}$	$< 5\times10^{-2}$
10	3RB-AS-R7	$(5.2\pm0.2)\times10^{-1}$	$(4.1\pm0.2)\times10^{-1}$	—
11	3RB-AS-R10	$(3.3\pm0.2)\times10^{-1}$	$(1.9\pm0.2)\times10^{-1}$	$< 5\times10^{-2}$
12	1RB-CR-R1	$(7.5\pm0.2)\times10^{0}$	$(4.4\pm0.9)\times10^{-1}$	$< 2\times10^{-1}$
16	1RB-CR-R5	$(5.0\pm0.7)\times10^{-1}$	$(3.4\pm0.5)\times10^{-1}$	$< 2\times10^{-1}$
18	1RB-CR-R7	$(2.8\pm0.2)\times10^{0}$	$< 4\times10^{-1}$	$< 3\times10^{-1}$
22	1RB-CR-R11	$(4.0\pm0.1)\times10^{1}$	$(1.1\pm0.1)\times10^{1}$	$(3.0\pm0.3)\times10^{-1}$
25	1RB-CR-R14	$(4.6\pm0.3)\times10^{1}$	$(3.7\pm0.2)\times10^{1}$	$< 6\times10^{0}$
26	1RB-OP-C1-1	$(1.3\pm0.1)\times10^{0}$	$(1.9\pm0.1)\times10^{0}$	$< 2\times10^{-1}$
27	1RB-OP-C1-2	$(5.3\pm0.1)\times10^{1}$	$(3.5\pm0.1)\times10^{1}$	$(3.2\pm0.1)\times10^{0}$
28	1RB-OP-D1-1	$(3.3\pm0.1)\times10^{2}$	$(4.6\pm0.2)\times10^{0}$	$(2.3\pm0.1)\times10^{1}$
29	1RB-OP-C2-1	$(9.9\pm0.5)\times10^{-1}$	$(3.8\pm0.3)\times10^{-1}$	$< 2\times10^{-1}$
30	1RB-OP-C2-2	$(3.9\pm0.1)\times10^{0}$	$(2.7\pm0.1)\times10^{1}$	$< 2\times10^{-1}$
31	1RB-OP-D2-1	$(1.8\pm0.1)\times10^{2}$	$(1.2\pm0.2)\times10^{0}$	$(9.4\pm0.3)\times10^{0}$

Table 5 Concentrations of alpha-particle-emitting nuclides on 11 March 2011 (Bq/g).

No.	Sample	^{238}Pu	$^{239+240}$Pu	^{241}Am	^{244}Cm
1	1U-05	$< 1\times10^{-2}$	$< 2\times10^{-2}$	$< 1\times10^{-2}$	$< 1\times10^{-2}$
2	3U-03	$< 1\times10^{-2}$	$< 2\times10^{-2}$	$< 1\times10^{-2}$	$< 1\times10^{-2}$
3	4U-07	$< 1\times10^{-2}$	$< 2\times10^{-2}$	$< 1\times10^{-2}$	$< 1\times10^{-2}$
24	1RB-CR-R13	$(6.0\pm1.1)\times10^{-1}$	$(1.6\pm0.6)\times10^{-1}$	$(1.6\pm0.4)\times10^{-1}$	$(1.6\pm0.4)\times10^{-1}$
28	1RB-OP-D1-1	$(9.4\pm1.7)\times10^{-1}$	$(3.0\pm0.9)\times10^{-1}$	$(4.8\pm0.7)\times10^{-1}$	$(2.5\pm0.6)\times10^{-1}$

3.2. Characteristics of rubble at each sampling location

Cesium-137 would be useful as a key nuclide when a simple and rapid radioactivity estimation is needed, because ^{137}Cs is the main radionuclide of FP and easily determined by nondestructive measurement. If the correlation between ^{137}Cs and nuclides that are difficult to measure is clarified, it is possible to combine the data calculated using a computer code and the values determined by the analysis. For this reason, the radioactivity ratios of ^{3}H, ^{14}C, ^{60}Co, ^{90}Sr, ^{238}Pu, $^{239+240}$Pu, ^{241}Am, and ^{244}Cm to ^{137}Cs determined in this study and previous study [3, 4] are plotted in Figure 5, and Figure 6.

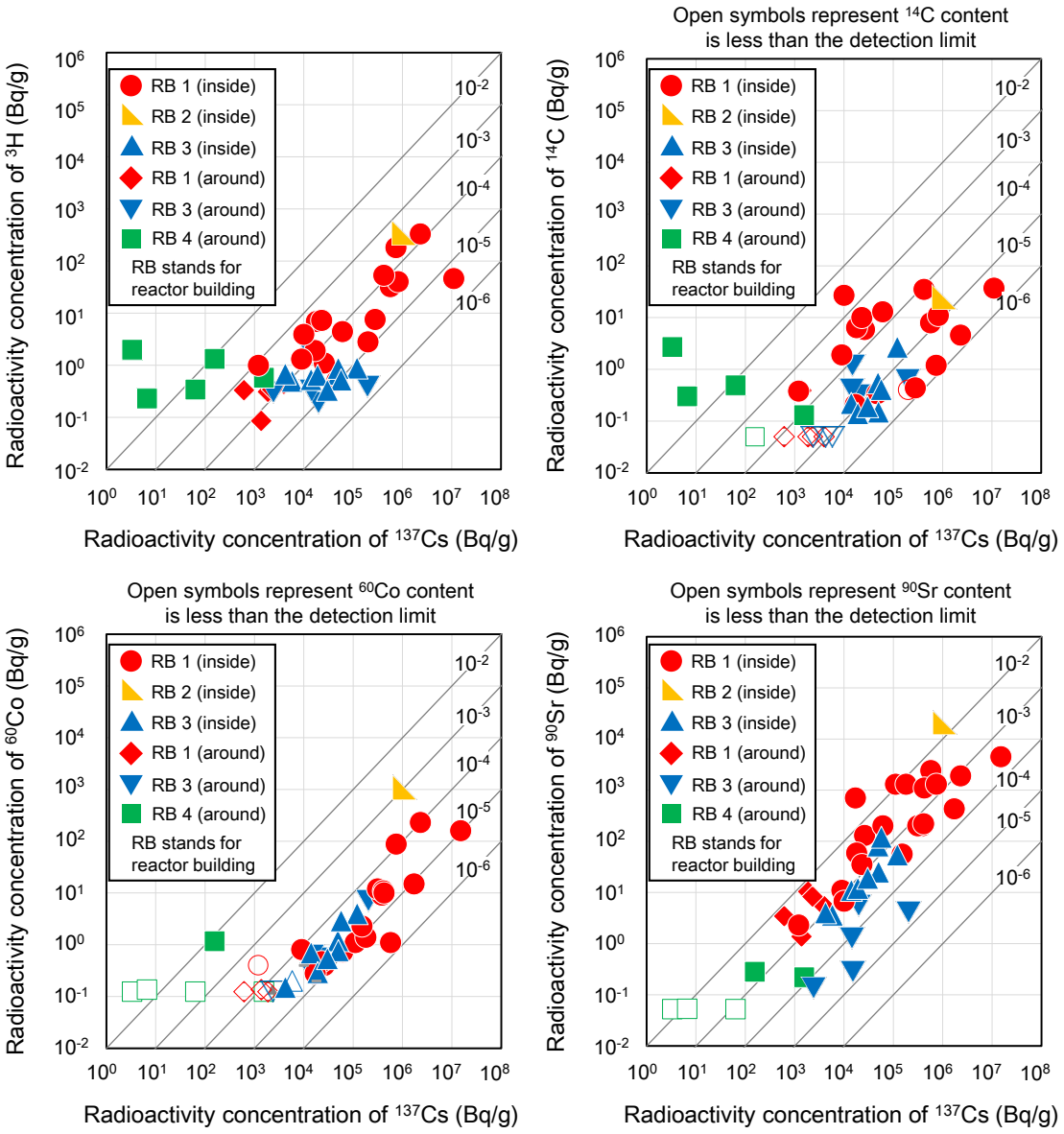

Figure 5. Correlation of concentration of ^{3}H, ^{14}C, ^{60}Co, and ^{90}Sr nuclides as a function of concentration of ^{137}Cs.

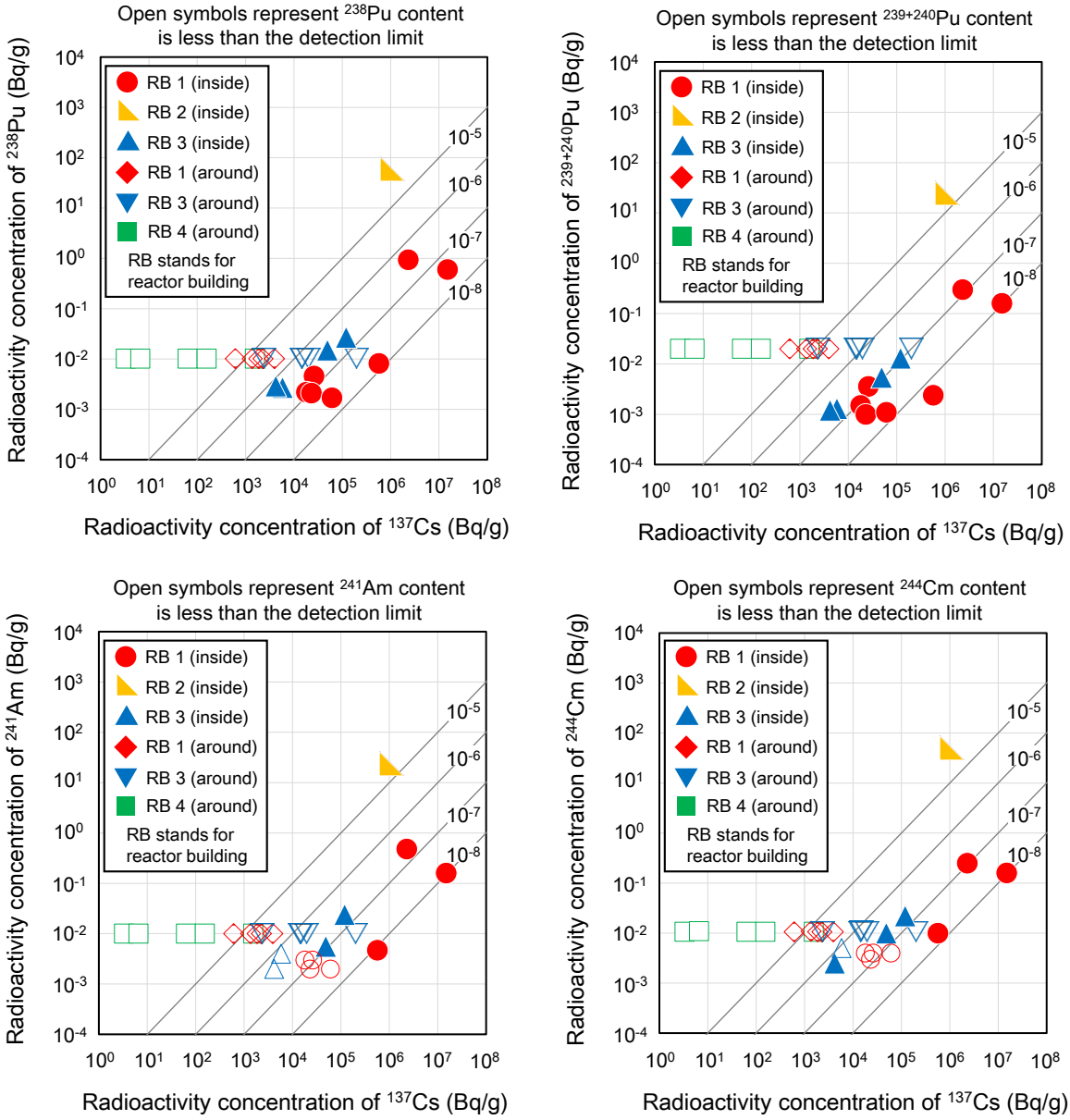

Figure 6. Correlation of concentration of alpha-particle-emitting nuclides as a function of concentration of ^{137}Cs.

As shown in Figure 5, rubble collected from inside reactor buildings were higher radioactivity concentration of ^{3}H and ^{14}C than rubble collected from around reactor buildings. Radioactivity ratios of ^{3}H to ^{137}Cs determined in this study varied ranging those determined in previous study [3, 4]. Each reactor buildings have similar ^{3}H/^{137}Cs radioactivity ratios in same order of magnitude. Radioactivity concentrations of ^{3}H and ^{14}C at Unit 1 were correlation to that of ^{137}Cs according to t-test since ^{3}H/^{137}Cs and ^{14}C/^{137}Cs radioactivity ratios were constant within where radioactivity concentrations of ^{137}Cs ranged from 10^{3} Bq/g to 10^{7} Bq/g. However radioactivity ratio of ^{3}H/^{137}Cs and ^{14}C/^{137}Cs at Unit 3 varied widely, ranging from 10^{-4} to 10^{-6}. This result indicated that radioactivity concentrations of ^{3}H and ^{14}C at Unit 3 were not correlation to that of ^{137}Cs, moreover result of t-test indicated same thing. Correlation between radioactivity concentrations of ^{3}H, and^{14}C to that of ^{137}Cs should be clarified by analyzing the rubble which had widely range of radioactivity concentration of ^{137}Cs.

Comparison of radioactivity concentrations of ^{60}Co at each Units, those for Units 1 and 3 were distributed around the line of 10^{-5}, which differs from that for Unit 2, where the ratios were lain around the line of 10^{-4}. The radioactivity concentrations of ^{60}Co at Units 1 and 3 were correlated to those of ^{137}Cs according to t-test. The radioactivity concentrations of ^{90}Sr were depended

on those of ^{137}Cs. The radioactivity ratios of ^{90}Sr to ^{137}Cs for Units 1, 2, and 3 were 2×10^{-3}, 2×10^{-2}, and 8×10^{-4}, respectively. The ^{90}Sr/^{137}Cs radioactivity ratios were high in order of Units 2, 1, and 3. The ^{90}Sr/^{137}Cs radioactivity ratios of rubble collected from around reactor buildings at Units 1, 3 ,and 4 were 3×10^{-3}, 4×10^{-5}, and 5×10^{-4}, respectively. Comparison of the rubble collected from Units 1 and 3, ^{90}Sr/^{137}Cs radioactivity ratios were consistent between the rubble collected from inside reactor buildings and that collected from inside reactor buildings within same order of magnitude. This result implied that the ^{90}Sr/^{137}Cs radioactivity ratio was consistent in each reactor buildings regardless of where collected from around or inside. Contaminated soils collected from outside of F1NPS was analyzed by S. Mishra et al.[6], and N. Kavasi et al. [7], and ^{90}Sr/^{137}Cs radioactivity ratios of those were distributed within 10^{-4} to 10^{-1}. The soils and the rubble had same range of ^{90}Sr/^{137}Cs radioactivity ratio. This result implied that the ^{90}Sr/^{137}Cs radioactivity ratio was consistent in onsite and offsite of F1NPS.

Figure 6 shows that correlation of concentration of alpha-particle-emitting nuclides as a function of concentration of ^{137}Cs. Radioactivity concentrations of ^{238}Pu and $^{239+240}$Pu were correlated to those of ^{137}Cs according to t-test. Americium-241 and Curium-244 were too little number of analyzed to estimate that radioactive concentration of ^{241}Am and ^{244}Cm was correlate to that of ^{137}Cs. However, as the radioactive concentration of ^{137}Cs increased, the radioactive concentration of ^{241}Am and ^{244}Cm increased. The analysis of ^{241}Am and ^{244}Cm should be continued to clarify that radioactive concentration of ^{241}Am and ^{244}Cm was correlate to that of ^{137}Cs.

3.3. Comparison of analytical data and calculated value

The radioactivity inventory of 335 radionuclides present in units 1-3 at the F1NPS was evaluated using the ORIGEN2 computer code [8]. The evaluated value was considered about the irradiated uranium pellet and the activated cladding tube of zirconium alloy in the core. Moreover radioactivity of ^{137}Cs, ^{90}Sr, and Pu released from reactor buildings was estimated by Ministry of Economy, Trade and Industry [9]. The estimated value was assumed as radioactive nuclides were released from stack or containment vessel to surroundings of reactor buildings. These values were compared with analytical data.

The radioactivity ratio of ^{60}Co/^{137}Cs evaluated using the ORIGEN2 for Units 1, 2, and 3 were 1.3×10^{-5}, 1.4×10^{-5}, and 1.4×10^{-5}, respectively [8]. That calculated by analytical data for Units 1, 2, and 3 were 2×10^{-5}, 1×10^{-3}, and 3×10^{-5}, respectively. Comparing radioactivity ratios of evaluation and these of analytical data, radioactivity ratios for Units 1 and 3 were within a same order of magnitude, and these of analytical data in Units 2 was two orders of magnitude higher than these of evaluation. Reactor buildings of Units 1 and 3 underwent a hydrogen explosion and reactor buildings of Unit 2 did not. The way of radioactive nuclides released from reactor buildings of Unit 2 was different to these of Units 1 and 3. The difference of ^{60}Co/^{137}Cs ratio between analytical data and estimation seemed to be due to the difference of accident situation.

The radioactivity ratio of ^{90}Sr/^{137}Cs evaluated using the ORIGEN2 for Units 1, 2, and 3 were 7.4×10^{-1}, 7.4×10^{-1}, and 7.5×10^{-1}, respectively [8]. These of calculation from analytical data for Units 1, 2, and 3 were 2×10^{-3}, 2×10^{-2}, and 8×10^{-4}, respectively. The evaluation of ^{90}Sr/^{137}Cs radioactivity ratios were 1 - 3 orders of magnitude higher than the ^{90}Sr/^{137}Cs radioactivity ratios calculated from analytical data. These results indicated that a release rate of ^{90}Sr radioactivity from reactor core to reactor buildings was lower than that of ^{137}Cs radioactivity. According to the estimation of the radioactivity released from the reactor buildings, the ^{90}Sr/^{137}Cs radioactivity ratios for Units 1, 2, and 3 were 1.0×10^{-2}, 3.4×10^{-3}, and 1.2×10^{-1}, respectively [9]. Considering that simulated conditions would vary calculation values ranging from one order of magnitude, the calculation of ^{90}Sr/^{137}Cs radioactivity ratios for Units 1 and 3 were within a range of permissible error.

Figure 6 shows that correlation of concentration of alpha-particle-emitting nuclides as a function of concentration of ^{137}Cs. The ^{238}Pu/^{137}Cs radioactivity ratios for Units 1, 2, and 3 were 8×10^{-8}, 6×10^{-5}, and 6×10^{-7}, respectively. According to the estimation of the radioactivity released from the reactor buildings, the ^{238}Pu/^{137}Cs radioactivity ratios for Units 1, 2, and 3 were 9.8×10^{-7}, 1.3×10^{-6}, and 3.5×10^{-7}, respectively [9]. The ^{238}Pu/^{137}Cs radioactivity ratios

of analytical data differed by one order of magnitude from those of calculation value. Considering that simulated conditions would vary calculation values ranging from one order of magnitude, the calculation of $^{238}Pu/^{137}Cs$ radioactivity ratios were within a range of permissible error. The $^{238}Pu/^{137}Cs$ radioactivity ratio of evaluated using the ORIGEN2 for Units 1, 2, and 3 were 2.3×10^{-2}, 1.8×10^{-2}, and 2.3×10^{-2}, respectively [8]. The $^{238}Pu/^{137}Cs$ radioactivity ratios of analytical data were 3 - 6 orders of magnitude lower than those of evaluation. As well as the $^{238}Pu/^{137}Cs$ radioactivity ratios, the $^{238}Pu/^{137}Cs$ radioactivity ratios of analytical data were lower than those of evaluation. Therefore a release rate of Pu radioactivity from reactor core to reactor buildings was lower than that of ^{137}Cs radioactivity. The radioactive concentration of Pu was as low as that released from global fall out. The $^{238}Pu/^{239+240}Pu$ radioactive ratio was compared in order to identify where Pu was released. The radioactivity ratio of ^{238}Pu to $^{239+240}Pu$ for Units 1, 2, and 3 were 2.1, 2.4 and 2.3, respectively. Those of plutonium ratio evaluated for Units 1, 2, and 3 in the reactor core were 2.9, 2.4, and 2.3, respectively [8]. On the other hand the radioactivity ratio of ^{238}Pu to $^{239+240}Pu$ from global fallout were 0.019 - 0.068 [10, 11]. Since plutonium ratios of analytical result were consistent to those of evaluation, we concluded that plutonium detected from rubble was released from F1NPS.

The radioactivity of ^{241}Am has increased for about seventy years as the ^{241}Pu radioisotope decayed. To compare analytical data to evaluation, The ^{241}Am radioactivity of reactor core was evaluated on 11 September 2017, then the evaluated value was converted into the radioactivity on 11 March 2011. The ^{241}Am radioactivity on 11 September 2017 was about five times higher than that on 11 March 2011. This result showed that the ^{241}Am radioisotope of about 20 percent existed in reactor core and that of about 80 percent was that the ^{241}Pu radioisotope decayed into ^{241}Am radioisotope. When a release rate of ^{241}Am radioactivity from reactor core to reactor buildings was similar to that of ^{238}Pu radioactivity, in most part of the ^{241}Am radioactivity which was detected by this study derived from ^{241}Pu radioisotope decayed. The evaluated value of the $^{241}Am/^{137}Cs$ radioactivity ratios for Units 1, 2, and 3 were 1.3×10^{-2}, 1.1×10^{-2}, and 1.4×10^{-2}, respectively. The $^{241}Am/^{137}Cs$ radioactivity ratios of analytical data for Units 1, 2, and 3 were 3×10^{-8}, 2×10^{-5}, and 2×10^{-7}, respectively. The $^{241}Am/^{137}Cs$ radioactivity ratios of analytical data were 3 - 6 orders of magnitude lower than those of estimation, as well as the $^{238}Pu/^{137}Cs$ radioactivity ratios. We could not identify ^{241}Am as ^{241}Am which was decayed by ^{241}Pu. In six years after from the accident, ^{241}Am radioactivity depended on released ^{241}Pu radioactivity We could not estimate that the release rate of Am was higher or lower than that of Pu.

The $^{244}Cm/^{137}Cs$ radioactivity ratios of analytical data for Units 1, 2, and 3 were 3×10^{-8}, 5×10^{-5}, and 3×10^{-7}, respectively. The evaluated value of the $^{244}Cm/^{137}Cs$ radioactivity ratios for Units 1, 2, and 3 were 1.3×10^{-2}, 1.3×10^{-2}, and 1.1×10^{-2}, respectively [8]. The $^{244}Cm/^{137}Cs$ radioactivity ratios of analytical data were 3 - 6 orders of magnitude lower than those of estimation, as well as the $^{238}Pu/^{137}Cs$ radioactivity ratios. This result implied that Cm and Pu had same release rate of radioactivity from reactor core to reactor buildings. Considering chemical property of Cm was similar to that of Am, the release rate of Am would be same order of magnitude as that of Pu and Cm.

4. Conclusion

To characterize the radioactivity composition of the rubble contaminated by the accident at the F1NPS, Our study presents the following conclusions:

- Radioactivity ratios of ^{60}Co and ^{90}Sr to ^{137}Cs were constant regardless of sampling location at reactor buildings of Unit 1.
- The radioactivity concentrations of ^{60}Co and ^{90}Sr were correlated with those of ^{137}Cs.
- The release rate of Pu, Am, and Cm was same order of magnitude.

Acknowledgment

The authors are grateful to Y. Okada, K. Sato, K. Kimiyama, T. Unno, M. Kajio, N. Yonekawa, S. Seki, T. Niiyama, S. Numayama, K. Suto, T. Tokunaga, K. Watanabe for their assistance in the experiment. This achievement is obtained from the Subsidy and Entrustment Project of Decommissioning and Contaminated Water Management by Ministry of Economy, Trade and Industry (METI).

References

[1] Ministry of Economy, Trade and Industry; “Storage conditions of the rubble and tree”, Available at: http://www.meti.go.jp/earthquake/nuclear/decommissioning/committee/osensuitaisakuteam/2017/07/3-04-02.pdf.

[2] K. KAMEO, A. SHIMADA, K. ISHIMORI, T. HARAGA, A. KATAYAMA, A. HOSHI, and Y. KAMEO; “Simple and Rapid Determination Methods for Low-level Radioactive Wastes Generated from Nuclear Research Facilities (Guidelines for Determination of Radioactive Waste Samples) ”, JAEA-Technology 2009-051, (2009).

[3] K. TANAKA, A. SHIMADA, A. HOSHI, M. YASUDA, M. OZAWA and Y. KAMEO; “Radiochemical analysis of rubble and trees collected from Fukushima Daiichi Nuclear Power Station”, J. Nucl. Sci. Tecnol., 51, pp.1033–1043 (2014).

[4] Y. SATO, K. TANAKA, T. UENO, K. ISHIMORI Y. KAMEO, “ Radiochemical Analysis of Rubble Collected from Fukushima Daiichi Nuclear Power Station”, Jpn. J. Health Phys., 51 (4), pp.209 - 217 (2016) , (in Japanese).

[5] K. KOBAYASHI, Y. IWAI, T. HAYASHI, T. YAMAGISHI; “Study of the behavior of tritiated water vapor in concrete materials”, journal of Nuclear Materials, 417, pp.1183-1186 (2011)

[6] S. MISHRA, S. K. SAHOO, H. ARAE, Y. WATANABE, JW. MIETELSKI; “Activity Ratio of Cesium, Strontium and Uranium with Site Specific Distribution Coefficients in Contaminated Soil near Vicinity of Fukushima Daiichi Nuclear Power Plant”, J. Chromatogr. Sep. Tech, 5, pp.250 - 256 (2014).

[7] N. KAVASI, S. K. SAHOO, A. SORIMACHI, S. TOKONAMI, T. AONO, S. YOSHIDA; Measurement of ^{90}Sr in soil samples affected by the Fukushima Daiichi Nuclear Power Plant accident, J. Radioanal. Nucl.Chem, 303 (2), pp.565-2570 (2015).

[8] K. NISHIHARA, H. IWAMOTO and K. SUYAMA. “Estimation of Fuel Compositions in Fukushima Daiichi Nuclear Power Plant”; JAEA-Data/code 2012-018 (2012).

[9] Ministry of Economy, Trade and Industry; “Evaluation of Unit-1, 2 and 3 reactor core state such of Fukushima Daiichi Nuclear Power Plant accident” Available at: http://www.meti.go.jp/earthquake/nuclear/pdf/20110606-1nisa.pdf,.

[10] H. FUJITA, H. WATANABE and M. TAKEISHI; “Annual variation of concentrations of Pu isotopes and Am in surface soil”, Cycle engineering Labs giho, 25, pp.45-48 (2004), (in Japanese).

[11] R. H. CLARKE, “Exposures resulting from nuclear explosions”, UNSCEAR REPORT , pp. 211-248 (1982) Available at:http://www.unscear.org/docs/reports/1982/1982-E_unscear .pdf